The Effect of Fuel/Air Mixture Composition on No Formation in Methane, Methanol and Methyl Formate Freely Propagating Flames

J. K. Tanui and P. N. Kioni

Abstract—In this study we have examined the effects of fuel/air mixtures composition on NO formation in methane/air, methanol/air, and methyl formate/air freely propagating flames. The flames have been numerically simulated at pressure of 1 bar and equivalence ratios (ϕ) from 0.7 to 1.3. Various chemical kinetic mechanisms have been employed and extensively tested so as to ensure validity of the results. A comparison of NO profiles for different equivalence ratios have been done for the three flames. The role of temperature in NO formation is clearly demonstrated in these profiles, with the NO profiles having direct correlation with temperature profiles. It has been established that there is a significant dependency of temperature for NO formation in methane/air as compared to the other flames. This is attributed to dominance of reaction; CH + N$_2$ $\longrightarrow$ HCN + N, which results in large amount of N atoms taking part in NO formation in temperature dependent Zeldovich thermal NO mechanism. On the other hand, the NO formation in methanol and methyl formate is mostly through reaction: NNH + O $\longrightarrow$ NH + NO, which is as a result of few CH radical and hence few N atoms responsible for NO formation in temperature dependent Zeldovich mechanism.

Keywords—Zeldovich mechanism; methane; methanol; methyl formate; NO

I. INTRODUCTION

The understanding of chemical pathways formation for NO$_x$ in a fuel oxidation is very important in determining the reduction techniques to be employed in a combustion system. In a combustion system, NO is formed in four different ways; thermal NO at high temperature flame zone or post-flame zone, prompt NO at low temperature flame zone, NO formed through the N$_2$O mechanism, and fuel NO produced by nitrogen portions in the fuel. The primary mechanism for thermal NO formation in a flame is attributed to extended Zeldovich mechanism [1] (O + N$_2$ $\longrightarrow$ NO + N, N + OH $\longrightarrow$ NO + H and N + O$_2$ $\longrightarrow$ NO + O). The Zeldovich reactions are strongly dependent on temperature. Prompt NO formation in the flame zone is associated with the presence of CH radical which react with nitrogen in the reaction: CH + N$_2$ $\longrightarrow$ HCN + N [2], [3]. N atom from the reaction then forms NO through reactions with OH and O in the Zeldovich mechanism. HCN reacts using various paths to form NCO and NH which subsequently form N atom responsible for NO formation.

J. Tanui, Department of Mechanical Engineering, Kimathi University College of Technology (corresponding author, phone: +254723503095; e-mail: josetanui@gmail.com).

P. N. Kioni, Kimathi University College of Technology (e-mail: ndirangukioni@yahoo.com).

This study reports on the effects of fuel/air mixtures composition on NO formation in methane/air, methanol/air, and methyl formate/air freely propagating flames. The investigation has been done for flames at pressure of 1 bar and equivalence ratios (ϕ) from 0.7 to 1.3. Various chemical kinetic mechanisms have been employed for the different fuels. Methane and methanol flames are computed using GRI-Mech 3.0 reaction mechanism [4], while methyl formate flame is computed by combining the Dooley *et al* [5] oxidation mechanism with the Leeds NOx oxidation mechanism [6]. All mechanisms used in this study have been widely validated and tested. GRI-Mech 3.0 reaction mechanism has been validated and tested in previous investigations [7], [8]. Dooley *et al* oxidation mechanism has also been validated in a wide range of conditions, viz, a variable pressure flow reactor, shock tube facility, outwardly propagating flames and burner stabilized flames [5], [9]. Similarly, Leeds NOx oxidation mechanism has been validated in flow reactors, perfectly stirred reactors and low pressure laminar flames by Hughes *et al*. [3].

II. NUMERICAL MODEL

We consider a laminar, one-dimensional premixed, freely propagating flame configuration as shown in Fig. 1. The cold fuel-air mixture enters the computational domain through the left boundary, and hot combustion products exit the domain through the right boundary. The governing equations and the
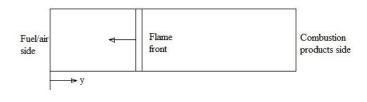

Fig. 1. Flow configuration for a freely propagating flame

equation of state for this configuration are as follows:

$$\frac{\partial \rho}{\partial t} + \frac{1}{A}\frac{\partial}{\partial y}(\rho V_y A) = 0; \tag{1}$$

$$\rho \left(\frac{\partial Y_i}{\partial t} + V_y \frac{\partial Y_i}{\partial y} \right) = -\frac{1}{A}\frac{\partial}{\partial y}(\rho Y_i V_i A) + w_i \quad i = 1, ..., N, \tag{2}$$

$$\rho C_p \left(\frac{\partial T}{\partial t} + V_y \frac{\partial T}{\partial y} \right) = \frac{1}{A} \frac{\partial}{\partial y} \left(\lambda A \frac{\partial T}{\partial y} \right)$$

$$- \frac{\partial T}{\partial y} \sum_{i=1}^{N} C_{pi} \rho Y_i V_i - \sum_{i=1}^{N} h_i w_i + \frac{dp}{dt}$$

$$- \frac{1}{A} \frac{\partial}{\partial y} (\mathbf{q}_R A) + A_s h_s (T - T_s), \qquad (3)$$

$$p = \rho RT \sum_{i=1}^{N} (Y_i / W_i). \qquad (4)$$

Here, A is spatially variable cross sectional area, ρ is density, t is time, is , p is pressure, R is universal gas constant, T is temperature, N is total number of species, V_y velocity in y direction, λ thermal conductivity, h_s is heat transfer coefficient between gas and solid phase, $\mathbf{q}_R$ is the radiant heat flux, A_s is local wetted surface area per unit void volume, T_s is temperature at the solid surface, while V_i, h_i, w_i, Y_i and W_i, C_{pi} represent diffusion velocity, specific enthalpy, rate of production by chemical reactions, mass fraction, molecular weight and specific heat capacity at constant pressure of species i.

The flames are numerically simulated using the RUN1DL code in the software package COSILAB [10]. Both central and one-sided difference (upwind) schemes are adopted in the discretization of first-order derivatives, while second-order derivatives are approximated by second order accurate central difference scheme. The time dependent version of the governing equations are first integrated with respect to time in steps starting with initial specified profiles, which should satisfy the equations at time level $m=0$ with $t=t^0 \equiv 0$. The solutions to governing equations are then sought at the subsequent time levels ($m = 1; t = t^1$), ($m = 2; t = t^2$),..., with $0 = t^0 < t^1 < t^2 < ... < t^m < ...$, where the superscript m is used to identify quantities at time level m. The integration is complete when either a specified time level m_{max} or time t_{max} is reached. The flames are fixed inside the computational domain at point y= 0.148 mm and T_0= 400 K so that the flames are steady in a frame of reference that moves with the flame speed. All the three flames have a constant pressure of 1 bar, a cold boundary temperature of 300 K, and zero temperature and species concentration profiles at the right boundary. Fuel/air mixture at the left boundary are varied from ϕ=0.7 to ϕ=1.3. The thermodynamic and transport properties for the species, which are in CHEMKIN format are obtained from Princeton University kinetic model databases [11] and GRI-Mech 3.0 databases [4].

III. Results and Discussion

The variation of fuel/air mixture in the different fuels investigated, was done to establish its impact on NO formation. Figs. 2-4 present results for each of the flames, while Figs. 6-12 compare NO formation at each equivalence ratio experimented ($\phi = 0.7$ to $\phi = 1.3$). For methane flame, the NO formation increases with increase in equivalence ratio. Methanol and methyl formate flames show a similar behavior, the NO formation increases with increase in equivalence ratio up to $\phi = 1.1$, and starts decreasing with further increase in

equivalence ratio. The role of temperature in NO formation is clearly demonstrated in these NO profiles. As depicted in Fig. 5, the maximum temperature attained by; methane/air is 2010 K at $\phi = 1.15$, methanol/air is 1973 K at $\phi = 1.1$, and methyl formate/air is 1964 K at $\phi = 1.2$. NO mole fraction profiles have direct correlation with temperature profiles.
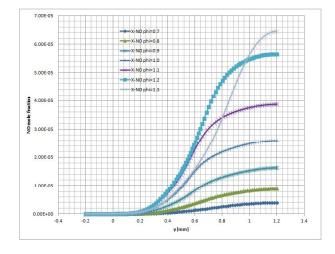

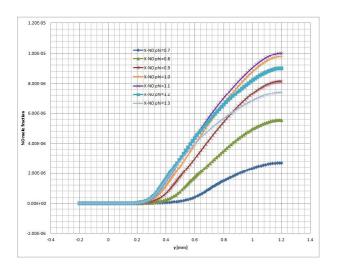Fig. 2. NO mole fraction profiles for various equivalence ratios of methane/air freely propagating flame

Fig. 3. NO mole fraction profiles for various equivalence ratios of methanol/air freely propagating flame

Figures 6-12 reveals a significant dependency of temperature for methane/air NO formation as compared to the other flames. This is attributed to the contribution of both prompt NO and thermal NO mechanism to the total NO formed in this particular flame. At low equivalence ratios, the maximum temperatures attained by all fuels are relatively low. Hence, the contribution by thermal NO become less significant. As the equivalence ratio is increased, temperature increases and the contribution by thermal NO becomes dominant. It is observed that increase in equivalence ratio does not increase the NO profiles significantly for methanol and methyl formate flames as it does for methane flame. The relevance of reaction; CH + N_2 $\longrightarrow$ HCN + N, which is a dominant initiation reaction responsible for NO formation in flames [2] [7], explains this
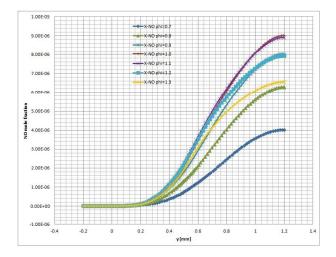
Fig. 4. NO mole fraction profiles for various equivalence ratios of methyl formate/air freely propagating flame
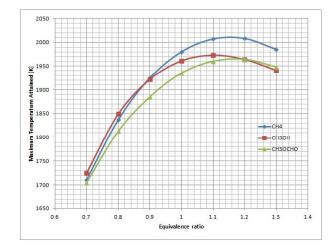

Fig. 7. Comparison of NO mole fraction profiles for the three flames at $\phi = 0.8$

Fig. 5. Maximum temperature attained by flames at different equivalence ratios

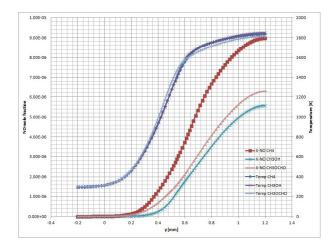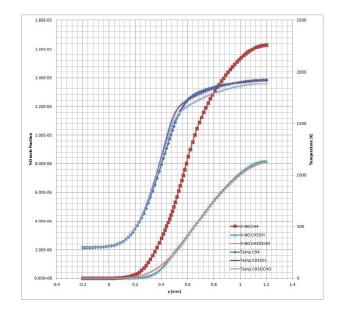Fig. 8. Comparison of NO mole fraction profiles for the three flames at $\phi = 0.9$

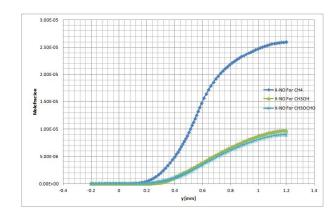Fig. 6. Comparison of NO mole fraction profiles for the three flames at $\phi = 0.7$

Fig. 9. Comparison of NO mole fraction profiles for the three flames at $\phi = 1.0$

observation. In methanol and methyl formate flames, there is less production of CH radical as compared to methane flame. This results in less amount of N atom, which is responsible for thermal NO formation through Zeldovich mechanism [1] ($O + N_2 \longrightarrow NO + N$, $N + OH \longrightarrow NO + H$ and $N + O_2 \longrightarrow NO + O$). The Zeldovich reactions are strongly dependent on
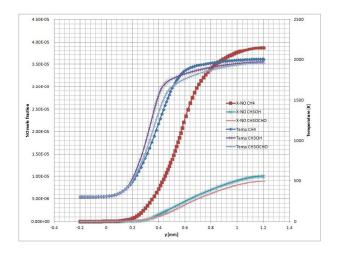
Fig. 10.   Comparison of NO mole fraction profiles for the three flames at $\phi = 1.1$
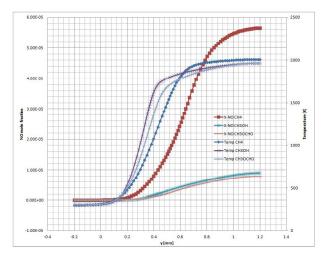

Fig. 11.   Comparison of NO mole fraction profiles for the three flames at $\phi = 1.2$
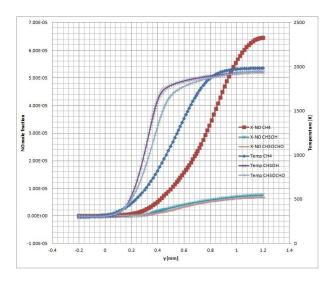

Fig. 12.   Comparison of NO mole fraction profiles for the three flames at $\phi = 1.3$

temperature. As a result, methane NO profiles are higher at high temperatures. On contrary, methanol and methyl formate

NO mole fraction profiles (whose main source is reaction; NNH + O $\longrightarrow$ NH + NO) are lower at high temperature.

IV. CONCLUSION

Methane/air, methanol/air and methyl formate/air freely propagating flames at pressure of 1 bar and equivalence ratios (ϕ) from 0.7 to 1.3 have been numerically simulated in this paper. The role of temperature in NO formation is clearly demonstrated in NO concentration profiles, with the NO profiles having direct correlation with temperature profiles. The results indicate that there is a significant dependency of temperature for NO formation in methane/air as compared to the other flames. This is explained by the relevance of reaction; CH + N$_2$ $\longrightarrow$ HCN + N, which is a dominant initiation reaction responsible for NO formation in flames. As a result, there is a large amount of N atoms from the reaction and the subsequent reactions involving HCN radical. N atoms then go into reaction with OH and O radicals in the temperature dependent Zeldovich mechanism. On the other hand, NO formation in methanol and methyl formate flames is less dependent on temperature. In these flames, there is less production of CH radical as compared to methane flame. This results in less amount of N atom, which is responsible for thermal NO formation through Zeldovich mechanism.

ACKNOWLEDGEMENT

REFERENCES

[1] I. Glassman and R. A. Yetter, *Combustion*. Elsevier, 2008.

[2] S. C. Li and F. A. Williams, "NOx formation in two-stage methane-air flames," *Combustion and flames*, vol. 118, pp. 399–414, 1999.

[3] K. J. Hughes, A.S. Tomlin, E. Hamparsounmian, W. Nimmo, I. G. Zsely, M. Ujvari, T. Turanyi, A. R. Clague, and M. J. Pilling, "An investigation of important gas-phase reactions of nitrogeneous species from simulation of experimental measurements in combustion systems," *combustion and flame*, vol. 124, pp. 573–589, 2001.

[4] G. P. Smith, D. M. Golden, M. Frenklach, N. W. Moriarty, B. Eiteneer, M. Goldenberg, C. T. Bowman, R. K. Hanson, S. Song, W. C. Gardener Jr., V. V. Lissianski, and Z. Qin, "Gri mech version 3.0," *http://www.me.berkeley.edu/grimech/ or.*

[5] S. Dooley, M. Chaos, M.P. Burke, Y. Stein, F.L. Dryer, C.A. Daly, V.P. Zhukov, and O. Finch, "An experimental and kinetic modeling study of methyl formate oxidation," *Proceedings of the European Combustion Meeting*, 2009.

[6] "Leeds NOx mechanism," *http://garfield.chem.elte.hu/Combustion/mechanisms/LeedsNOx20.dat*, 1999.

[7] S. Naha and S. K. Aggarwal, "Fuel effects on NOx emmisions in partially premixed flames," *Combustion and flames*, vol. 139, pp. 90–105, 2004.

[8] R. S. Barlow, A. N. Karpetis, J. H. Frank, and J. Y. Chen, "Scalar profiles and NO formation in laminar opposed-flow partially premixed methane/air flames," *Combustion and flame*, vol. 127, pp. 2102–2118, 2001.

[9] S. Dooley, F.L. Dryer, B. Yang, T.A. Cool, T. Kasper, and N. Hansen, "An experimental and kinetic modeling study of methyl formate oxidation at low pressure flames," *Combustion and Flame Journal*, vol. 158, 2011.

[10] "COSILAB software package," *www.rotexo.com/cms/index.php*.

[11] *http://www.princeton.edu/mae/people/faculty/dryer/homepage/kineticmodels/methylformate/.*